Reactive power control and performance analysis of doubly fed induction generatorin micro grid

Syed Sarfaraz Nawaz[1], Sandipam Tara Kalyani[2]

[1]Department of Electrical and Electronics Engineering, Gokaraju Rangaraju Institute of Engineering and Technology, Hyderabad, India
[2]Department of Electrical and Electronics Engineering, Jawaharlal Nehru Technological University, Hyderabad, India

Article Info

ABSTRACT

For both financial and environmental considerations, the power system includes a large number of solar and wind generating plants. In reality, wind energy has always been used using a doubly fed induction generator (DFIG) based variable speed wind turbine. This study examines the effectiveness of indirect control of a doubly fed induction generator for closed loop reactive power adjustment. A wind energy conversion system with continuous grid power's design, analysis, and MATLAB simulation are also covered. For DFIG to work reliably and be controlled to ensure stability for the power system, a seamless transition mode change is required. The horizontal axis wind turbine technology provides the necessary reactive power into the grid under all unexpected circumstances. The concept of DFIG mathematical modelling is covered. Various simulated outputs at loading circumstances are shown, along with separate control of active and reactive powers and variations in prime mover speed and excitation. This study examines the performance enhancement of DFIG using its grid-based proportional integral (PI), proportional integral derivative (PID), and fractional order proportional integral derivative (FOPID) controllers. Based on the thorough simulation findings, the type of control system that gives the efficient performance of DFIG in grid is ultimately decided. These simulation results demonstrate how the suggested controllers outperform the current controllers in terms of improving system performance.

Corresponding Author:

Syed Sarfaraz Nawaz
Department of Electrical and Electronics Engineering
GokarajuRangaraju Institute of Engineering and Technology
Hyderabad, India
Email: sarfaraz86nawaz@gmail.com

1. INTRODUCTION

The concept of free waste production, saving andstrong electric power arises as a result ofthe only source of natural energy, fossil fuelsshrinkage, global warming and gas emissions. Renewableenergy sources play an important role in solving most past problems. Doubly fed induction generator (DFIG) can increase productivity, lower costs and losses, modify the power feature, offer variable speed, and regulate both real and reactive power [1]-[4]. The doubly fed induction generator is one of the most popular generators utilised in high power wind generation (DFIG). The rotor of the DFIG is connected to the grid via a back-to-back power electronic converter [5]-[10], whilst the stator is connected directly to the micro grid.

The grid is directly connected to the DFIG stator windings, while the grid is connected to the rotor windings via back-to-back converters, rotor side converters, and grid side converters (GSC) [11]–[16]. These controller controlspower and dc link voltage respectively. The capacity to operate across a wide range of

wind speeds and the reduction in size and cost of power converters are two advantages of this type of machine [17]-[19]. Recent studies have focused on the use of sophisticated and robust controllers like regulation, pole placement and tracking (RST), Sliding mode controller, backstepping, and active disturbance rejection control active disturbance rejection control (ADRC) to enhance DFIG control and extract the most dependable and steady power from it. However, this kind of controllers has several drawbacks when dealing with grid defaults [20]-[24]. The control method used which is intended to control the outputpower provided grid. Such common controlsas a proportional-integral (PI) controller and proportional integral derivative (PID) is used because of its simplicity solid structure and performance. However, the maindisadvantages of these conventional controllers (PI and PID) arethat their performance is deteriorating due to changesoperating system conditions causeddemand increase [25], [26].

The major goals of this study are to develop a comprehensive MATLAB/Simulink mathematical model. Additionally, it provides a thorough comparison of the simulation results for PI, PID, and FOPID controllers. The auto tuner in MATLAB/Simulink is used to obtain the parameters of PI and PID controllers. Using grey wolf optimisation (GWO), the FOPID controller's parameters are obtained (GWO). These outcomes demonstrate how effective the suggested controllers perform.

The DFIG block diagram is shown in Section 2. Then, in Section 3, the DFIG converter control operation is described. Section 4 presents the Simulink model of the DFIG with the added load. Section 5 discusses the Simulink MATLAB model of the DFIG based on PI, PID, or FOPID controller. Section 6 presents a mathematical model of the DFIG, while section 7 discusses the design of the controllers. Section 8 offers the simulation findings. The paper concludes with its conclusions in the end.

2.   BLOCK DIAGRAM OF DFIG

Figure 1 depicts the DFIG system's fundamental block diagram. The stator and rotor are coupled by the power electronic control system. The stator side converter's primary function is to maintain a steady DC link voltage. The back-to-back converter's reactive power consumption can be easily managed to keep the power factor at unity. Although the converter's capacity for power distribution reduces inaccuracy to a ratio of 1/4 of the output power of turbines, it nevertheless functions as a further device for compensation.
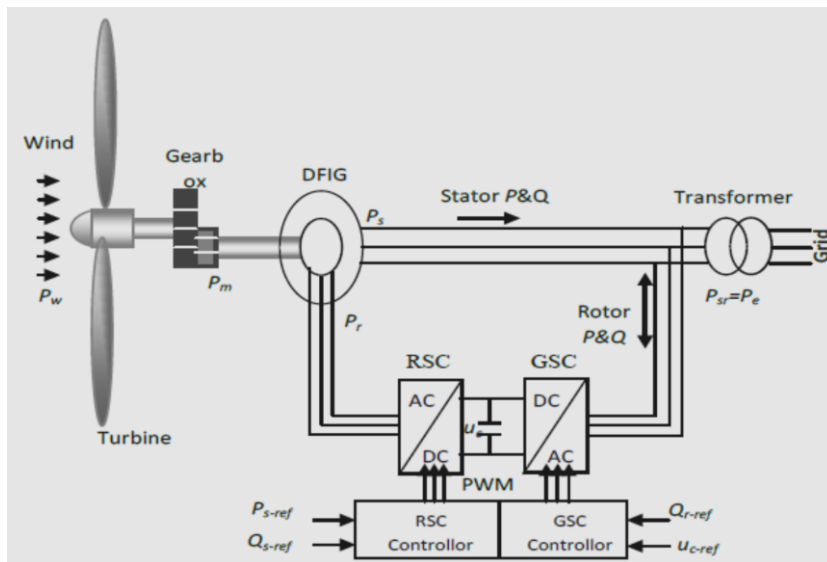

Figure 1. Block diagram representation of DFIG

The asynchronous machine's stator is directly connected to the grid, or the supply. The rotor of the asynchronous machine and the DC machine are combined in this lab model. When the direct current (DC) machine is running at a different speed, the rotor side converter acts as an inverter or adaptor. The identical procedure will be used by the grid side converter. Utilizing a prime mover (DC machine) running at varied speeds, the armature voltage control approach is utilised to achieve different DFIG speeds. The capacitor bank is connected to the stator terminals of the input device to provide the magnetic field required for the machine to function.

2.1. DFIG's open loop model

The induction machine in the laboratory model is driven by a DC motor to operate at sub-synchronous, synchronous, and super-synchronous speeds. Figure 2 depicts a diagram of the open loop work block when the provided three-phase design is substituted with a three-phase designed source on the rotor. By directly altering the frequency of the systematic energy source, this model only allows for the adjustment of the generated EMF frequency across all stator windings.

However, in this arrangement, the systematic power source's frequency is manually changed to ensure that the EMFs that drive the stator have a frequency that is equivalent to the supply frequency at various wind speeds (50 Hz). It is difficult to estimate which frequency supply stator voltages will be available at 50 Hz frequency. Figure 3 depicts the Simulink model for the DFIG's open-loop control.
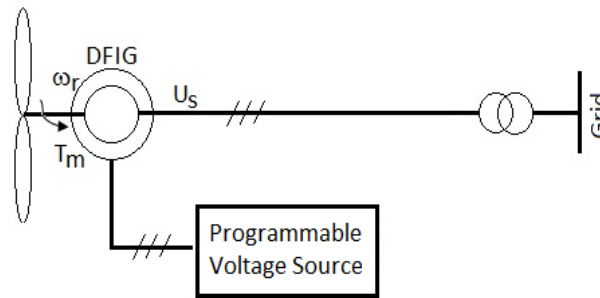

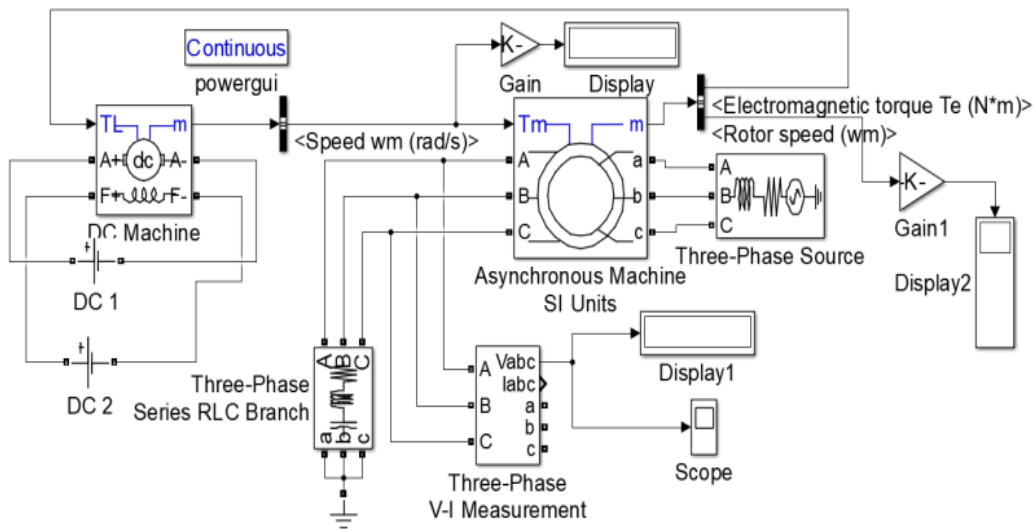Figure 2. Block diagram of open loop control of DFIG

Figure 3. Simulink model of DFIG's open loop model

2.2. Closed loop model of DFIG

To prevent this, the voltage supplied to the rotor at frequency f must be altered continually until the side voltages on the stator have a frequency of 50 Hz. An internal carrier wave (triangular wave) of around 1080 Hz is used as the internal reference signal for a pulse width modulation (PWM) generator that produces the pulses for these variables. An inverter that was created utilising MOSFET switches is used to do this. The closed DFIG loop's operation is represented by the block diagram in Figure 4. Figure 5 depicts the Simulink model with the GSC and rotor side converter (RSC) for the closed DFIG loop operation. This model replicates oscillations in frequency and stator power output at various speeds.
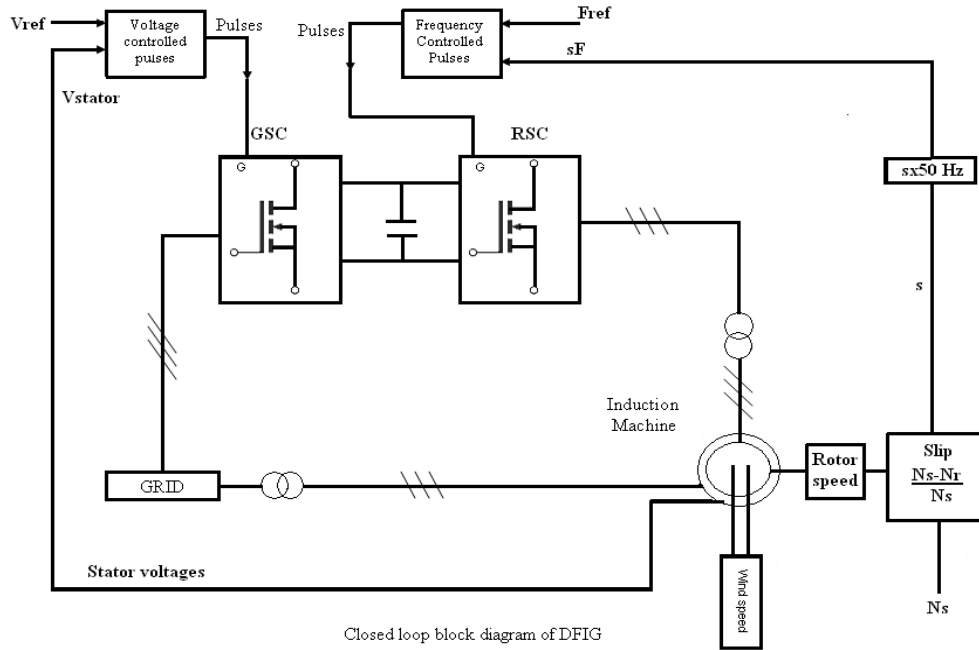
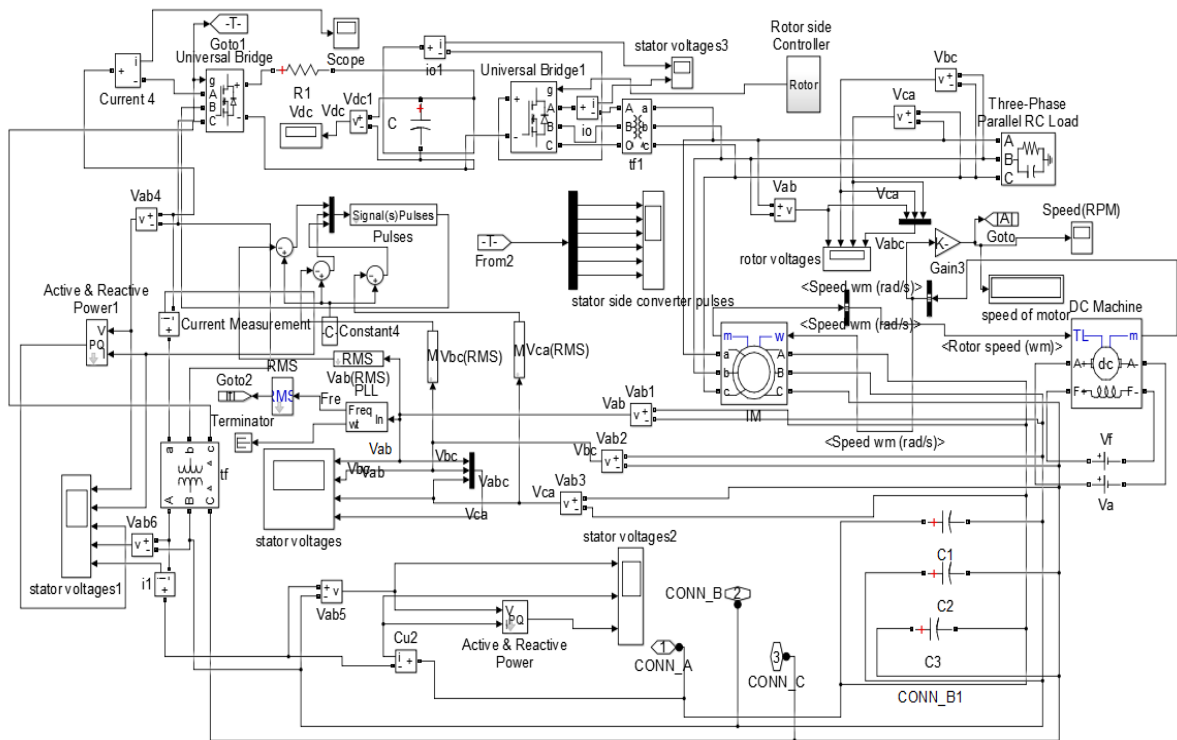Figure 4. Block diagram of closed loop control of DFIG

Figure 5. Simulink model of closed loop control of DFIG

3. CONVERTER CONTROL OPERATION

3.1. Grid side converter

According to Figure 6, the Simulink GSC model generates switching pulses by sending a switching signal to Simulink's PWM production block. The PWM pulse generator receives these varied signals as a result of comparing the reference voltage with the stator's output voltages. Metal oxide semiconductor field effect transistors (MOSFETs) are the switches in use here.
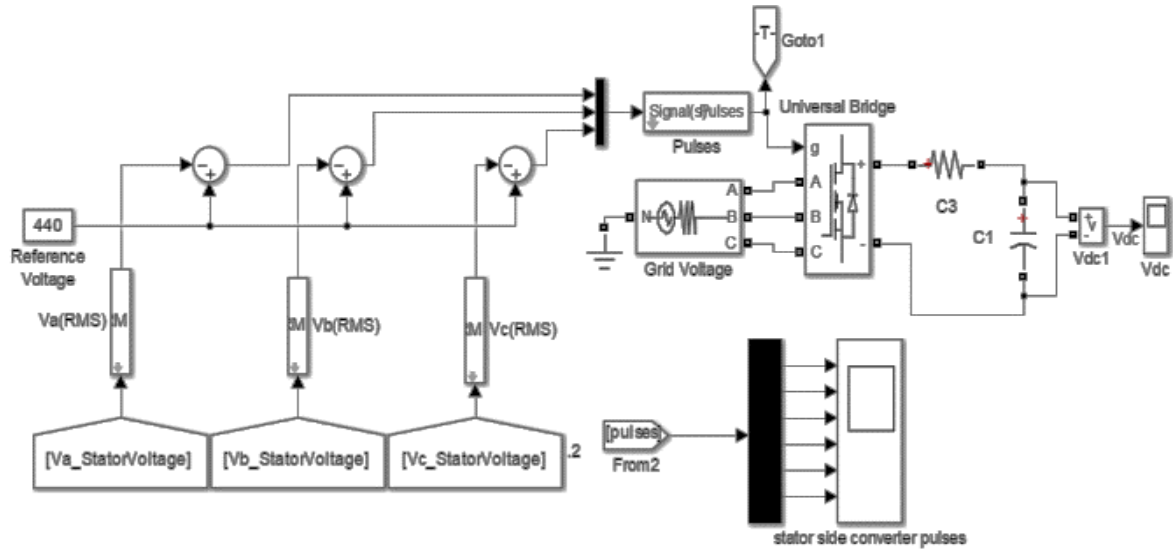
Figure 6. Simulink model of GSC

3.2. Rotor side converter

Figure 7 offers a block representation of the RSC. The converter construction is similar to the GSC, but the signal switching reference signal is provided by the PWM pulse generator, which is made using a slide frequency. Slip frequency (f'=sf) generates reference signals, or three sine waves, which are supplied as input to the PWM generator. In order to control the stator frequency, the frequency of the output stator voltages is taken as a response. A smoother frequency is created using the difference in frequency. This reference is used by the PWM block generator.
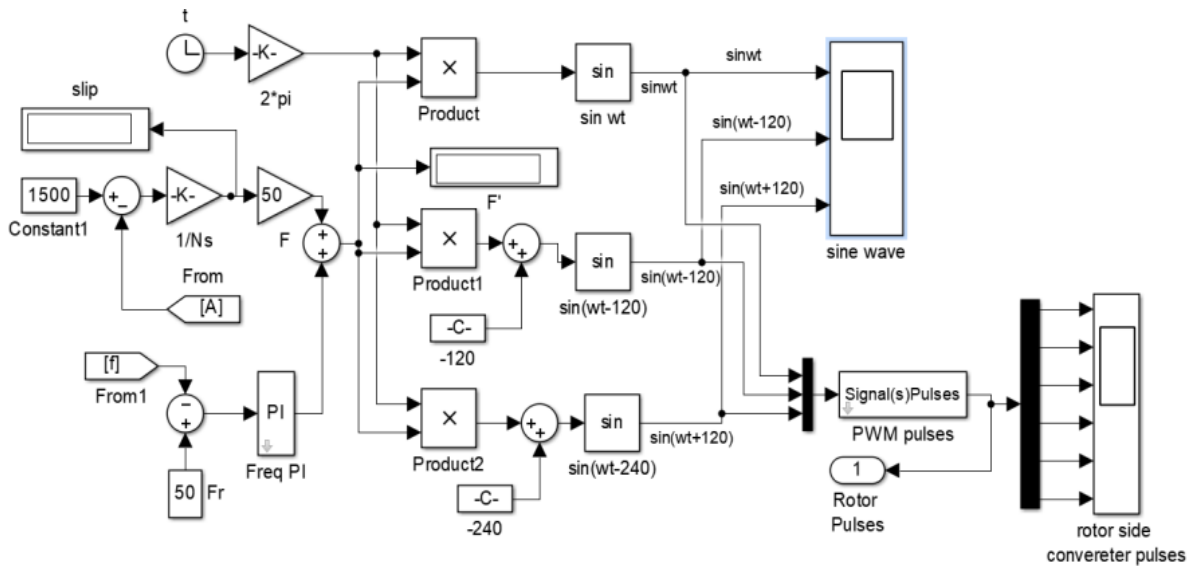

Figure 7. Simulink model of RSC

4. SIMULINK MODEL OF DFIG WITH ADDITIONAL LOAD

The simulation of the DFIG connected grid converter and the whole model are shown in Figure 8. The voltage across the grid decreases when an unexpected load (inductive loads) is applied because too much power is being drawn. The DFIG succeeds in compensating this active force. According to this concept, after a new load is added to the grid, the DFIG is connected, creating new effects.
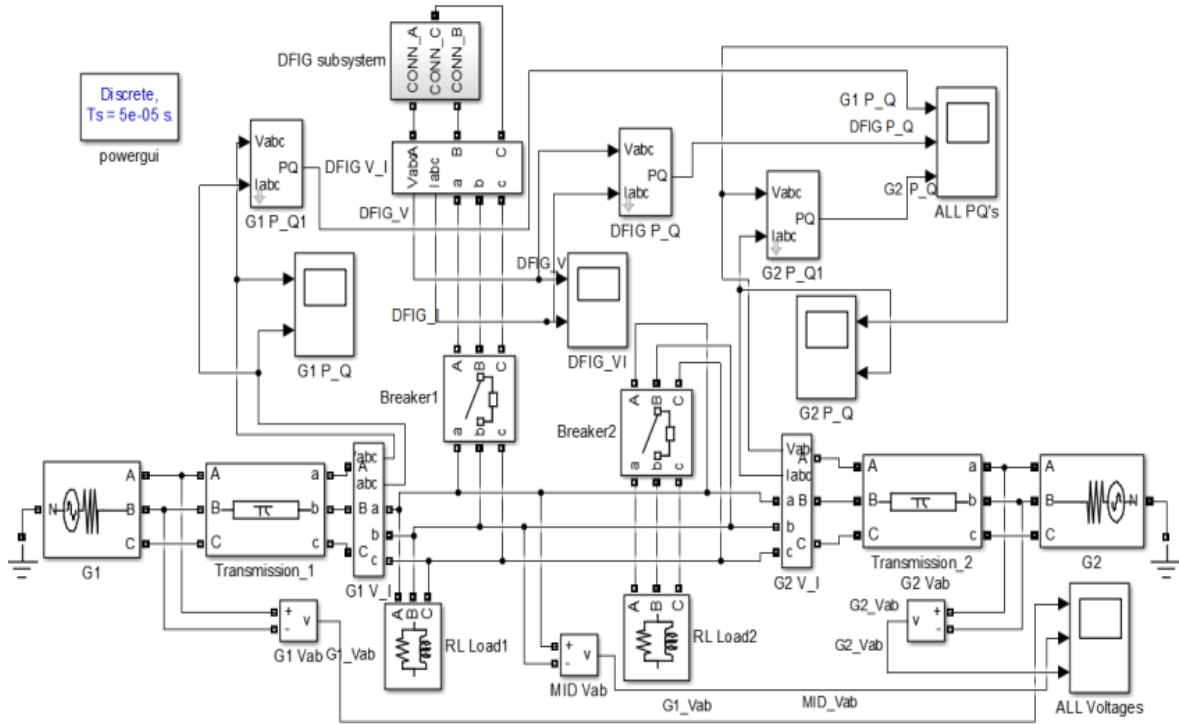
Figure 8. DFIG connected to the grid using a Simulink model with an additional load

5. DFIG's SIMULINK MODEL WITH PI, PID, OR FOPID CONTROLLER

A Simulink model of a DFIG connected to a grid by a PI, PID, or FOPID controller is shown in Figure 9. In the DFIG system, several controllers are put between capacitor voltage and reactive power to boost efficiency. Initially PIcontroller is used for the simulation purpose followed by PID controller. The results of FOPID is compared with those of PI and PID controllers. It is seen that the performance of FOPID controller outperforms as compared to other controllers.
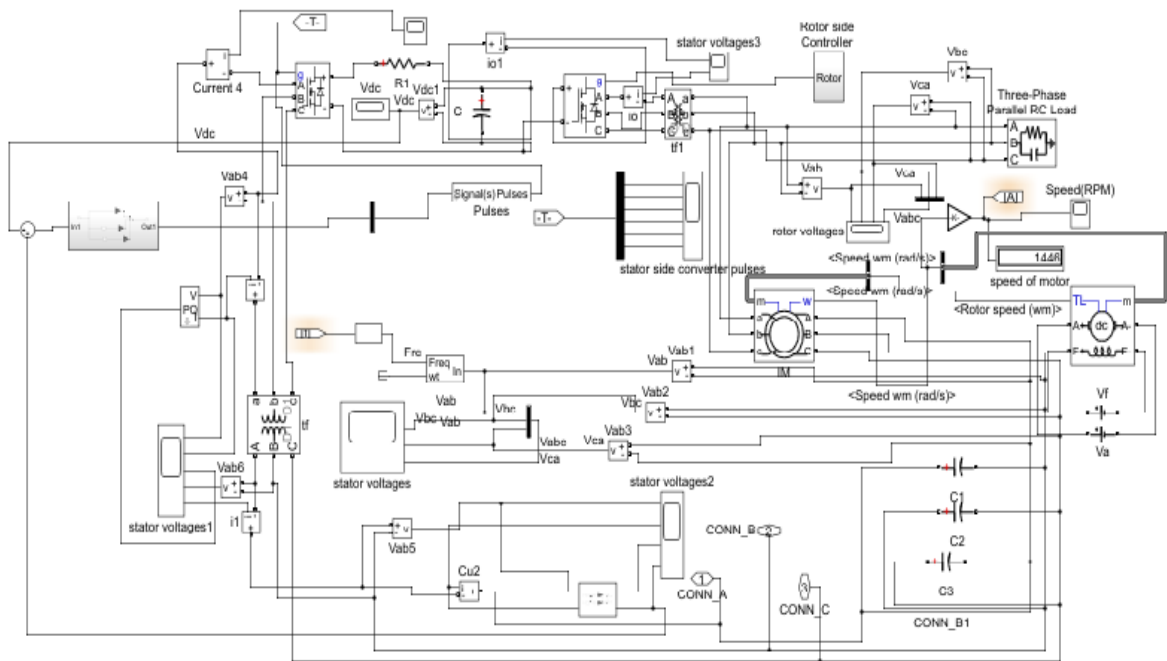

Figure 9. DFIG's Simulink model with various controller

6. DFIG's MATHEMATICAL MODEL

In this article, only the stator reference frame is taken into consideration for all equations (stator and rotor). Voltage and stator flux can be depicted as (1).

$$\left.\begin{array}{l} \vec{V_s} = R_s\vec{I_s} + \frac{d\vec{\psi_s}}{dt} \\ \vec{\psi_r} = L_r\vec{I_r} + L_m\vec{I_s} \end{array}\right\} \tag{1}$$

Voltage and flux of rotor can be represented as (2).

$$\left.\begin{array}{l} \vec{V_r} = R_r\vec{I_r} + \frac{d\vec{\psi_r}}{dt} - j\omega_m\vec{\psi_r} \\ \vec{\psi_r} = L_r\vec{I_r} + L_m\vec{I_s} \end{array}\right\} \tag{2}$$

From (1) and (2):

$$\frac{d\vec{I_s}}{dt} = \frac{1}{L_rL_s - L_m^2}\left\{ L_r\vec{V_s} - (L_rR_s + j\omega_m L_m^2)\vec{I_s} - L_m\left(\vec{V_r} + (j\omega_m L_r - R_r)\vec{I_r}\right)\right\} \tag{3}$$

$$\frac{d\vec{I_r}}{dt} = \frac{1}{L_rL_s - L_m^2}\left\{ L_s\vec{V_r} - (R_r - j\omega_m L_r)\vec{I_r}L_s - L_m\left(\vec{V_s} + (j\omega_m L_s + R_s)\vec{I_r}\right)\right\} \tag{4}$$

Rotor voltage of DFIG.

$$V_r = R_r\vec{I_r} + sj\omega_s L_r\vec{I_r} + sj\omega_s L_m\left(\vec{I_r} + \vec{I_s}\right) \tag{5}$$

Stator voltage of DFIG.

$$V_s = R_s\vec{I_s} + sj\omega_s L_{\omega s}\vec{I_s} + sj\omega_s L_m\left(\vec{I_r} + \vec{I_s}\right) \tag{6}$$

Where $s = \frac{\omega_s - \omega_m}{\omega_m}$

$$\text{Stator Active Power is } P_s = \frac{3}{2}Re\left(\vec{V_s} * \vec{I_s^*}\right) \tag{7}$$

$$\text{Rotor Real Power is } P_r = \frac{3}{2}Re\left(\vec{V_r} * \vec{I_r} *\right) \tag{8}$$

7. CONTROLLERS DESIGN

The PI controller is considered in the form of $G_{pi}(s) = K_p + \frac{K_i}{s}$. The PID control structure is considered as $G_{pid}(s) = K_c\left(1 + \frac{1}{T_i s} + T_d s\right)$. The FOPID controller's transfer function can be expressed as $G_{fopid}(s) = K_p + \frac{K_i}{s^\lambda} + K_d s^\mu$. The parameters of PI and PID controllers are obtained using auto tuning block in MATLAB/Simulink. However, the grey wolf optimisation (GWO) technique is used to acquire the settings of the FOPID controller. A meta-heuristic method called the grey wolf optimizer was developed because wolves, as described in [27], are members of the Canidae family. The power of the wolf determines how long wolves have survived by searching for prey. The powerful wolf has a better chance of surviving. They typically hunt in packs of five to twelve wolves. At the wolf level, it affects the likelihood of catching the prey. The GWO algorithm's hunting procedure mimics wolves' sequence levels. The group leader, denoted as alpha (α), is given the highest level. Beta (β), the wolf rank below a leader, is given the next highest level.

The third level is this one. The delta wolf (δ)is a key player in the search because it inspires other wolves to follow an open-minded leader. The final level of the class, known as omega (ω), and its movement toward animals depend on the placement of the ranks mentioned above, are shared by several wolves. The social hierarchy and GWO algorithm's pseudocodes can be found in [28]-[30].

8.   SIMULATIONS RESULTS

The waveforms shown in Figure 10 represent the PWM pulses given to the GSC. The waveforms shown in Figure 11 represent the PWM pulses given to the RSC. The waveforms shown in Figure 12 represent the dc output voltage across DC link.
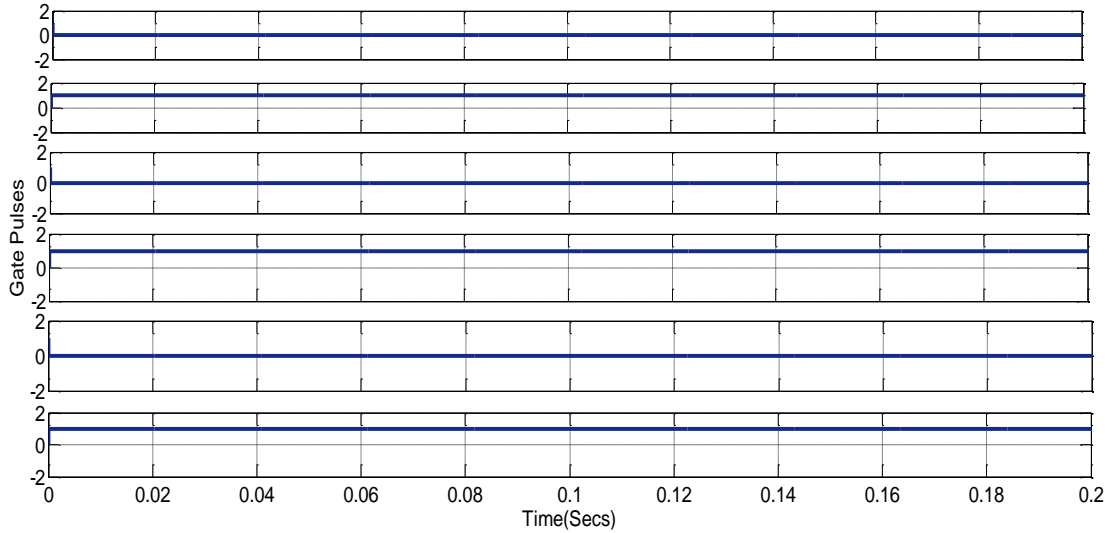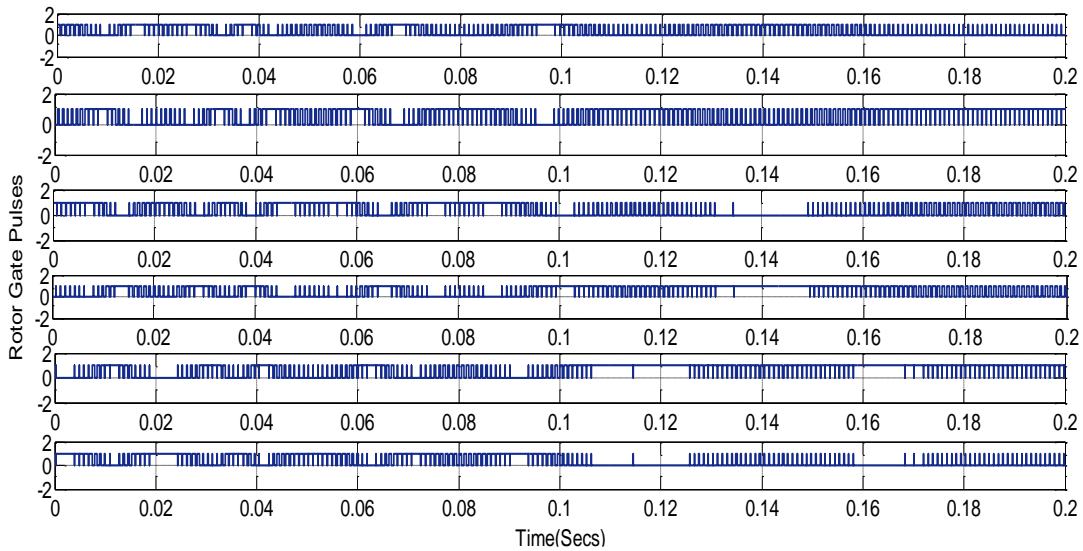

Figure 10. Stator side pulse waveforms

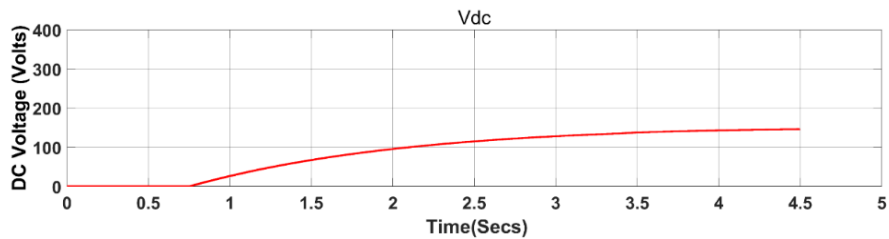Figure 11. Rotor side pulses' waveforms

Figure 12. DC voltage output waveforms

Figures 13, 14, and 15 for sub-synchronous, synchronous, and super-synchronous circumstances, respectively, illustrate simulated waveforms for rotor speeds. The stator voltages of DFIG are shown by the waveforms in Figure 16. The waveforms in Figure 17 depict the grid and DFIG's real and reactive power when the load is applied. Grid voltages at pre and post DFIG operated for grid 1, midpoint and grid 2 are shown in Figure 18.
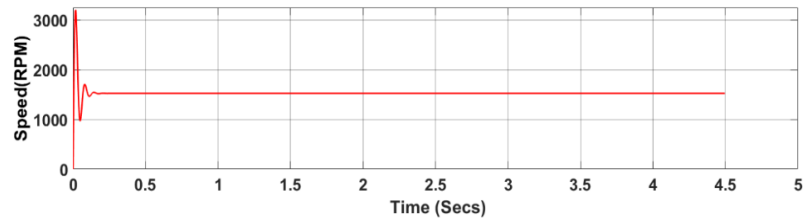

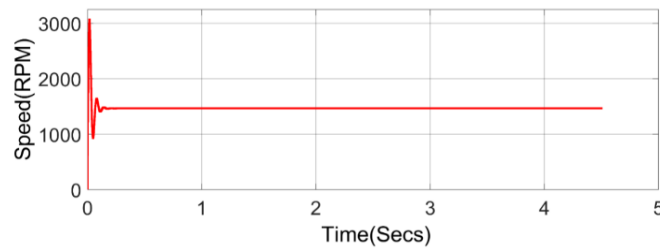Figure 13. At 1400 rpm, a wave forms for the rotor speed

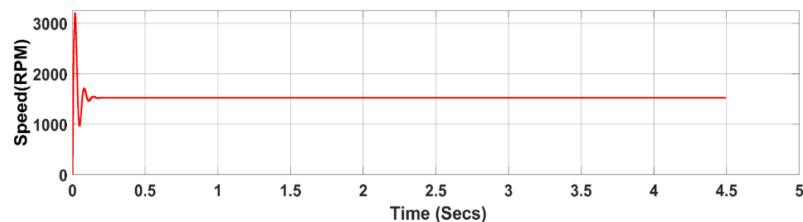Figure 14. At 1500 rpm, a wave forms for the rotor speed

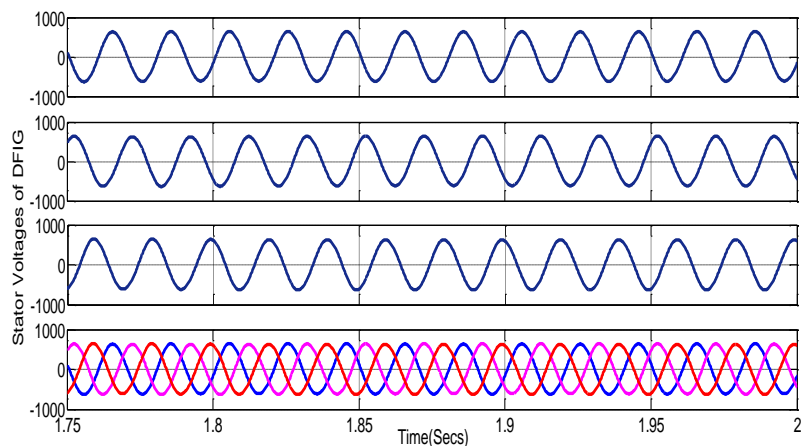Figure 15. At 1600 rpm, a wave forms for the rotor speed

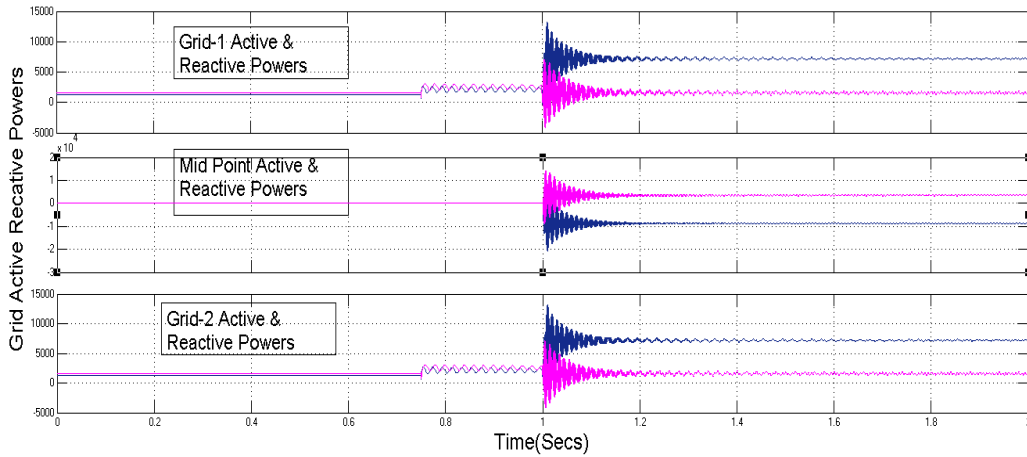Figure 16. Wave forms for stator side voltages

Figure 17. Real and reactive power grid and DFIG without controllers
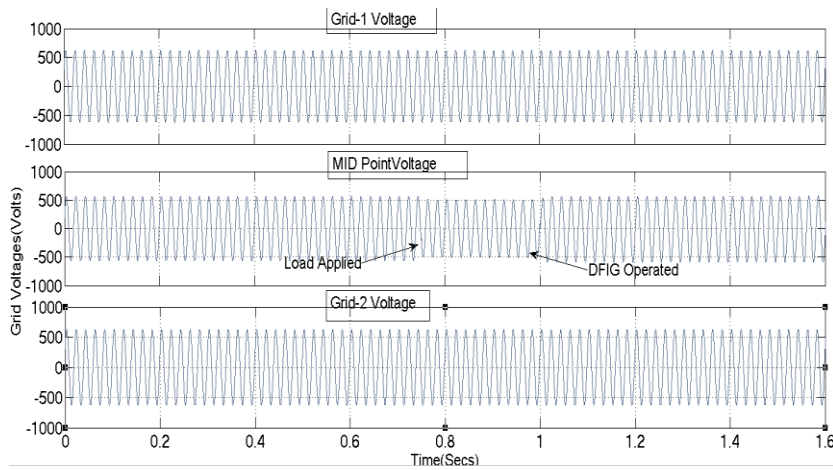
Figure 18. Grid side voltages

The specifications for DFIG system are considered as: X_m= 54.07 Ω, L_s=0.00589 H, R_s=50 Ω, L_m= 0.1722 H, L_r= 0.005839 H, R_r= 45 Ω, L_g=0.0006 H, X_g= 0.1884 Ω,R_g= 0.0001 Ω, V_r=180 V, C_{dc}= 1× 10^{-2} F, V_s=440 V RMS, i_{qs}=0.8 A, i_{ds}=1.95 A, i_{qr}=0.09 A, i_{dr}=0.155 A, V_{dc}=45 V, i_{qg}=1.76 A, i_{dg}=1.481 A, V_{qr}=97 V, V_{qg}=230.56 V, V_{qs}=245 V, V_{ds}=365.48 V, V_{dr}=151.6 V, V_{dg}=374.75 V, L_{rr}= 0.17839 H, L_{ss}= 0.17809 H,$ω_s$= 314 rad/sec, J=0.05 kg m^2, f=50 Hz.

Figure 19. Waveforms for grid and DFIG real and reactive power with PI controller

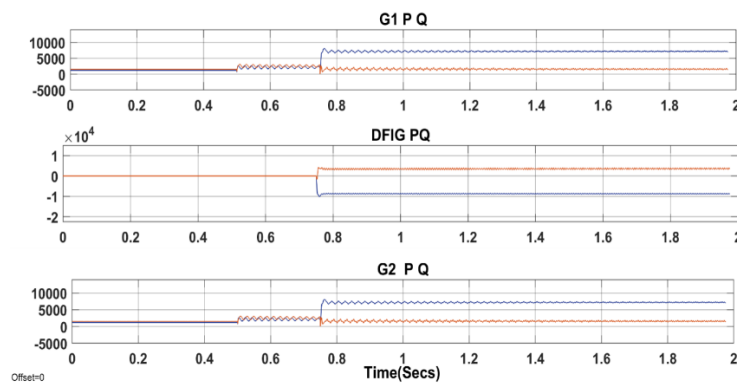The parameters of the PI controller are found as $K_p = 4.37$, $K_i = 32.24$ using the PI tuner in MATLAB/Simulink to meet the requirements for the DFIG system. These PID controller parameters are determined using the PID tuner in MATLAB/Simulink: $K_c = 220.43$, $T_i = 12.58$, $T_d = 5.32$. Additionally, the GWO algorithm yields the following results for the FOPID controller's controller settings: $K_p = 190.16$, $K_i = 49.97$, $K_d = 2.28$, $\lambda = 1.27$, and $\mu = 0.98$. Figure 19 depicts areal and reactive power grid, a DFIG, and a PI controller.

Apparent power generated for synchronous speedusing PI controller is shown in Figure 20. Figure 21 displays the apparent power produced for synchronous speed using a PID controller. Figure 22 displays the apparent power produced for synchronous speed using a FOPID controller. In comparison to PI and PID controllers, the suggested FOPID technique has a shorter settling period and less oscillations. The FOPID control technique offers higher control performance, as can be observed in Table 1.
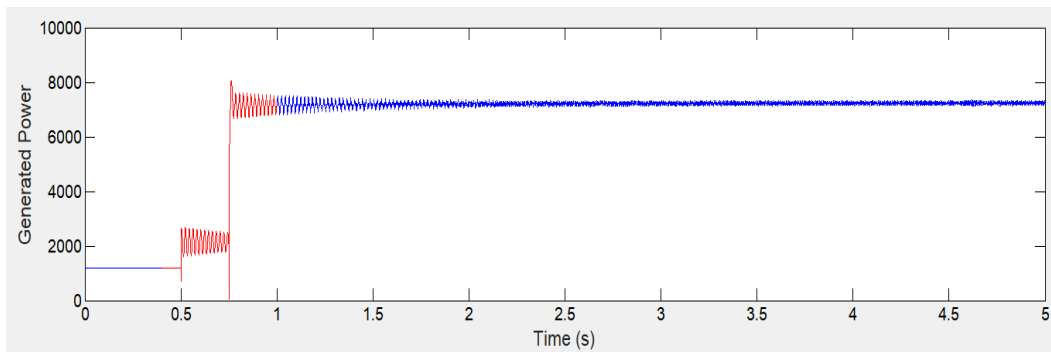

Figure 20. At 1500 RPM, power produced using a PI controller
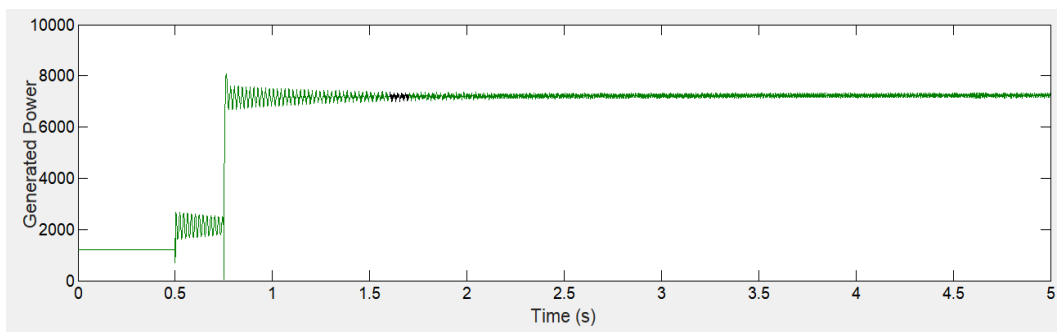

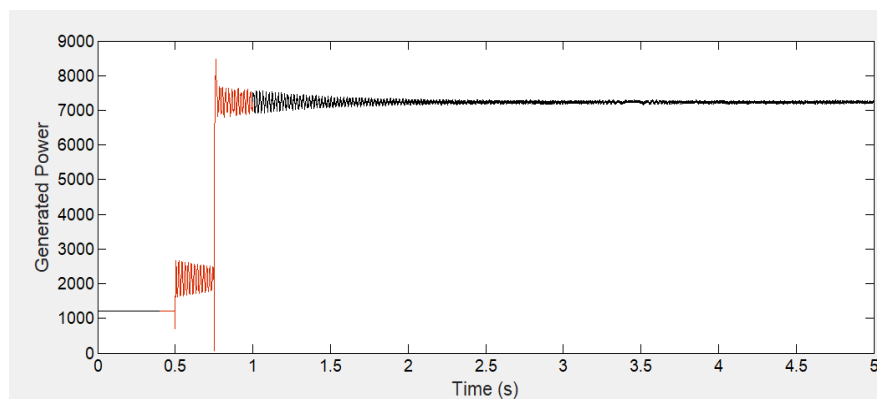Figure 21. At 1500 RPM, power produced using a PID controller

Figure 22. Power generated using FOPID controller at 1500 RPM

Table 1. Performance criteria

Parameters	Settling time (Sec)
PI controller	4
PID controller	3.5
FOPID controller	2

9. CONCLUSIONS

A DFIG's performance analysis has been described. This document presents the DFIG's mathematical modelling. Using a MATLAB simulation model, the values of generated power, DC voltage, wind speed, and grid side are identified. It has been useful to employ a dual power supply DFIG system connected to the power grid via an AC-DC-AC converter to increase the efficiency of power conversion due to the advancement of power electronics. When connected to the grid with the appropriate converter control systems, the DFIG system showed to be the most dependable and stable one, according to the results. Analyses are done on real and reactive power both with and without controllers. It is established that the FOPID controller performs better than other traditional controllers.

REFERENCES

[1]   L. Xu and W. Cheng, "Torque and reactive power control of a doubly fed induction machine by position sensorless scheme," *IEEE Transactions on Industry Applications*, vol. 31, no. 3, pp. 636–642, 1995, doi: 10.1109/28.382126.
[2]   C. Rawal and A. Mulla, "An AC-AC converter for doubly fed induction generator driven by wind turbine," *International Journal of Scientific and Research Publications*, vol. 4, no. 12, pp. 1–7, 2014.
[3]   F. A. Elkader, F. A. Khalifa, A. E. Kalas, and B. El Elnaghi, "Controller performance of DFIG Based wind energy conversion sysem," in *16th International Middle- East Power Systems Conference -MEPCON'2014 Ain Shams University, Cairo, Egypt*, 2014, pp. 23–25.
[4]   J. P. Mishra, D. Hore, and A. Rahman, "Fuzzy logic based improved active and reactive power control operation of DFIG for wind power generation," in *8th International Conference on Power Electronics - ECCE Asia: "Green World with Power Electronics", ICPE 2011-ECCE Asia*, May 2011, pp. 654–661, doi: 10.1109/ICPE.2011.5944631.
[5]   D. Yang, X. Wang, F. Liu, K. Xin, Y. Liu, and F. Blaabjerg, "Adaptive reactive power control of PV power plants for improved power transfer capability under ultra-weak grid conditions," *IEEE Transactions on Smart Grid*, vol. 10, no. 2, pp. 1269–1279, Mar. 2019, doi: 10.1109/TSG.2017.2762332.
[6]   W. Choi, W. Lee, and B. Sarlioglu, "Reactive power compensation of grid-connected inverter in vehicle-to-grid application to mitigate balanced grid voltage sag," in *IEEE Power and Energy Society General Meeting*, Jul. 2016, vol. 2016-November, pp. 1–5, doi: 10.1109/PESGM.2016.7741910.
[7]   M. El Moursi, G. Joos, and C. Abbey, "A secondary voltage control strategy for transmission level interconnection of wind generation," *IEEE Transactions on Power Electronics*, vol. 23, no. 3, pp. 1178–1190, May 2008, doi: 10.1109/TPEL.2008.921195.
[8]   T. Brekken, N. Mohan, and T. Undeland, "Control of a doubly-fed induction wind generator under unbalanced grid voltage conditions," in *2005 European Conference on Power Electronics and Applications*, 2005, vol. 2005, pp. 10 pp.-P.10, doi: 10.1109/epe.2005.219315.
[9]   S. Engelhardt, I. Erlich, C. Feltes, J. Kretschmann, and F. Shewarega, "Reactive power capability of wind turbines based on doubly fed induction generators," *IEEE Transactions on Energy Conversion*, vol. 26, no. 1, pp. 364–372, Mar. 2011, doi: 10.1109/TEC.2010.2081365.
[10] M. Kayikçi and J. V. Milanović, "Reactive power control strategies for DFIG-based plants," *IEEE Transactions on Energy Conversion*, vol. 22, no. 2, pp. 389–396, Jun. 2007, doi: 10.1109/TEC.2006.874215.
[11] R. Pena, J. C. Clare, and G. M. Asher, "Doubly fed induction generator using back-to-back PWM converters and its application to variablespeed wind-energy generation," *IEE Proceedings: Electric Power Applications*, vol. 143, no. 3, pp. 231–241, 1996, doi: 10.1049/ip-epa:19960288.
[12] Y. Mishra, S. Mishra, M. Tripathy, N. Senroy, and Z. Y. Dong, "Improving stability of a DFIG-based wind power system with tuned damping controller," *IEEE Transactions on Energy Conversion*, vol. 24, no. 3, pp. 650–660, Sep. 2009, doi: 10.1109/TEC.2009.2016034.
[13] W. Du, J. Bi, J. Cao, and H. F. Wang, "A method to examine the impact of grid connection of the DFIGs on power system electromechanical oscillation modes," *IEEE Transactions on Power Systems*, vol. 31, no. 5, pp. 3775–3784, Sep. 2016, doi: 10.1109/TPWRS.2015.2494082.
[14] G. Abad, J. López, M. A. Rodríguez, L. Marroyo, and G. Iwanski, *Doubly fed induction machine*, Hoboken, NJ, USA: John Wiley & Sons, Inc., 2011.
[15] M. Tazil *et al.*, "Three-phase doubly fed induction generators: An overview," *IET Electric Power Applications*, vol. 4, no. 2, pp. 75–89, 2010, doi: 10.1049/iet-epa.2009.0071.
[16] E. Vittal, M. O'Malley, and A. Keane, "Rotor angle stability with high penetrations of wind generation," *IEEE Transactions on Power Systems*, vol. 27, no. 1, pp. 353–362, Feb. 2012, doi: 10.1109/TPWRS.2011.2161097.
[17] S. Ghosh and S. Kamalasadan, "An energy function-based optimal control strategy for output stabilization of integrated DFIG-flywheel energy storage system," *IEEE Transactions on Smart Grid*, vol. 8, no. 4, pp. 1922–1931, Jul. 2017, doi: 10.1109/TSG.2015.2510866.
[18] I. Erlich, J. Kretschmann, J. Fortmann, S. Mueller-Engelhardt, and H. Wrede, "Modeling of wind turbines based on doubly-fed induction generators for power system stability studies," *IEEE Transactions on Power Systems*, vol. 22, no. 3, pp. 909–919, Aug. 2007, doi: 10.1109/TPWRS.2007.901607.
[19] R. Bhushan and K. Chatterjee, "Mathematical modeling and control of DFIG-based wind energy system by using optimized linear quadratic regulator weight matrices," *International Transactions on Electrical Energy Systems*, vol. 27, no. 11, p. e2416, Nov. 2017, doi: 10.1002/etep.2416.

[20] P. H. Huang, M. S. El Moursi, W. Xiao, and J. L. Kirtley, "Subsynchronous resonance mitigation for series-compensated dfig-based wind farm by using two-degree-of-freedom control strategy," *IEEE Transactions on Power Systems*, vol. 30, no. 3, pp. 1442–1454, May 2015, doi: 10.1109/TPWRS.2014.2348175.

[21] A. E. Shakarami Mahmood Reza, Joorabian Mahmood, "Enhancement fault ride-through of DFIG with applications of ISM control for balance and unbalance voltage sag," *Computational Intelligence in Electrical Engineering*, vol. 10, no. 3, pp. 41–60, 2018, doi: 10.22108/ISEE.2018.112687.1147.

[22] G. S. Kaloi, J. Wang, and M. H. Baloch, "Dynamic modeling and control of DFIG for wind energy conversion system using feedback linearization," *Journal of Electrical Engineering and Technology*, vol. 11, no. 5, pp. 1137–1146, Sep. 2016, doi: 10.5370/JEET.2016.11.5.1137.

[23] R. K. Patnaik, P. K. Dash, and K. Mahapatra, "Adaptive terminal sliding mode power control of DFIG based wind energy conversion system for stability enhancement," *International Transactions on Electrical Energy Systems*, vol. 26, no. 4, pp. 750–782, Apr. 2016, doi: 10.1002/etep.2105.

[24] N. Govindarajan and D. Raghavan, "Doubly fed induction generator based wind turbine with adaptive neuro fuzzy inference system controller," *Asian Journal of Scientific Research*, vol. 7, no. 1, pp. 45–55, Dec. 2014, doi: 10.3923/ajsr.2014.45.55.

[25] N. Jain, G. Parmar, R. Gupta, and I. Khanam, "Performance evaluation of GWO/PID approach in control of ball hoop system with different objective functions and perturbation," *Cogent Engineering*, vol. 5, no. 1, Jan. 2018, doi: 10.1080/23311916.2018.1465328.

[26] R. Sitharthan and M. Geethanjali, "An adaptive Elman neural network with C-PSO learning algorithm based pitch angle controller for DFIG based WECS," *JVC/Journal of Vibration and Control*, vol. 23, no. 5, pp. 716–730, Mar. 2017, doi: 10.1177/1077546315585038.

[27] S. Mirjalili, S. M. Mirjalili, and A. Lewis, "Grey Wolf Optimizer," *Advances in Engineering Software*, vol. 69, pp. 46–61, Mar. 2014, doi: 10.1016/j.advengsoft.2013.12.007.

[28] V. Soni, G. Parmar, M. Kumar, and S. Panda, "HGWO-PS optimized 2DOF-PID controller for non reheat two areas interconnected thermal power plants: A comparative study," in *1st IEEE International Conference on Power Electronics, Intelligent Control and Energy Systems, ICPEICES 2016*, Jul. 2017, pp. 1–6, doi: 10.1109/ICPEICES.2016.7853131.

[29] B. Bhanupradeep and D. D. G. Padhan, "Design of fractional order PID (FOPID) for load frequency control via IMC & Grey wolf algorithm (GWO), for a non-reheated power system by comparing with the big bang big crunch (BBBC) optimization," *International Journal of Recent Technology and Engineering (IJRTE)*, vol. 9, no. 1, pp. 1253–1260, May 2020, doi: 10.35940/ijrte.a1626.059120.

[30] J. Agarwal, G. Parmar, R. Gupta, and A. Sikander, "Analysis of grey wolf optimizer based fractional order PID controller in speed control of DC motor," *Microsystem Technologies*, vol. 24, no. 12, pp. 4997–5006, Dec. 2018, doi: 10.1007/s00542-018-3920-4.

BIOGRAPHIES OF AUTHORS

Syed Sarfaraz Nawaz 🆔 📇 sc ⬡ pursuing PhD from JNTUH. He had done his M.Tech with DISTINCTION in 2010 from GRIET Hyderabad and his B.Tech FIRST CLASS in 2007 from SSITS affiliated to JNTUH. He had overall experience of 12 years. He is familiar with software's like MATLAB, LABVIEW, EAGLE, KEIL, E-Tap Software, Proteus, Multisim, VISIM, PSIM etc and worked on DSPACE1104, F28086/7 DSP Control boards, PCI6221 Control Card and TI control boards. His areas of interest are power electronics, power systems, and machines. He can be contacted at email: sarfaraz86nawaz@gmail.com.

Dr. Sandipam Tara Kalyani 🆔 📇 sc ⬡ completed her Ph. D in FACTS, from JNTU Hyderabad in 2008. Her areas of interests are Power Electronics, Control Systems, Fundamentals of Electrical Engineering, Energy Systems, Power Systems. She worked as Assistant Director, Academic Staff College, University Grants Commission, JNTUH. As she had strong work experience, she also served as Deputy Director, Academic Staff College. she worked as Controller of Examinations for JNTUH University. She is now Director of UIIC. She can be contacted at email: tarakalyani@gmail.com.